

The magnetic properties of $\text{BiY}_2\text{Fe}_5\text{O}_{12}$ nanoparticles doped with Cr ions

Biao Dong · Hua Yang · Yuming Cui ·
Lianxiang Yu · Shouhua Feng

Received: 5 July 2005 / Accepted: 4 January 2006 / Published online: 26 March 2007
© Springer Science+Business Media, LLC 2007

Abstract $\text{BiY}_2\text{Cr}_x\text{Fe}_{5-x}\text{O}_{12}$ ($x = 0, 0.05, 0.1, 0.2, 0.3$) nanocrystals were synthesized by using a sol-gel method. Samples were characterized by the powder X-ray diffraction (XRD), the thermal gravity analysis (TGA) and the differential thermal analysis (DTA), the vibrating sample magnetometer (VSM) and Mössbauer spectrums. The average sizes of the particles were determined by the Scherrer's formula. The special M_s and Mössbauer spectra of $\text{BiY}_2\text{Cr}_x\text{Fe}_{5-x}\text{O}_{12}$ nanocrystals are researched at room temperature. It is seen that the special M_s s of samples are initially increased with increasing Cr^{3+} content ($x < 0.1$), and decreased with increasing content of Cr^{3+} ions ($x > 0.1$).

Introduction

Rare-earth iron garnet particles are very attractive objects of magnetic research. This is because they are single magnetic domain and accordingly their properties and their mutual interaction can be studied without magnetic domain effects. These materials have a uniquely defined cation distribution and do not present any site inversion problems which can arise in other ferrites. From an industrial

viewpoint, they are applicable to media for high-density magnetic or magneto-optical information storage. Among the magnetic material, polycrystalline yttrium iron garnets and substituted ones have received a great deal of attraction in laser, microwave devices and magneto-optics.

Recently, the bismuth–yttrium iron garnet (Bi–YIG) was found that it has enhanced Faraday rotation effect of one order of magnitude larger than that of YIG [1]. The Bi–YIG nano-particles is a most attractive material for magneto-optical devices [1, 2]. Y.H. Jeon's study [3] on Bi–YIG/epoxy hybrids show that they are promising materials for magneto-optical devices. Furthermore, replacement of Y^{3+} ions by Bi^{3+} ions can decrease the crystallization temperature for 100 °C to 300 °C in contrast to YIG [2, 4].

In this paper, the single-phase polycrystalline $\text{BiY}_2\text{Fe}_5\text{O}_{12}$ nanoparticles were synthesized by a sol-gel method. Basing on the well properties of $\text{BiY}_2\text{Fe}_5\text{O}_{12}$, we enhance the magnetic properties of the $\text{BiY}_2\text{Fe}_5\text{O}_{12}$ nanoparticles via further substitution of Fe^{3+} ions by Cr^{3+} ions. It is researched that the effect of the Cr^{3+} content x on magnetic properties of samples by the vibrating sample magnetometer and Mössbauer spectra.

Experimental

Polycrystalline samples with the general formula $\text{BiY}_2\text{Cr}_x\text{Fe}_{5-x}\text{O}_{12}$ ($x = 0.0, 0.05, 0.1, 0.2, 0.3$) were initially prepared from a solution of analytically pure grade $\text{Bi}(\text{NO}_3)_3 \cdot 5\text{H}_2\text{O}$, $\text{Fe}(\text{NO}_3)_3 \cdot 9\text{H}_2\text{O}$, $\text{Y}(\text{NO}_3)_3 \cdot 9\text{H}_2\text{O}$, and citric acid in appropriate stoichiometric ratios at 80 °C until gelation. Gels were dried at 100 °C for 36 h to form the precursors which were further preheated at 450 °C for 1 h and calcined at 850 °C, 920 °C and 1000 °C for 3 h.

B. Dong · H. Yang (✉) · Y. Cui · L. Yu ·
S. Feng
College of Chemistry, Jilin University, Changchun 130023,
P.R. China
e-mail: huayang86@sina.com

S. Feng
State Key Laboratory of Inorganic Synthesis and Preparative
Chemistry, Jilin University, Changchun 130023, P.R. China

The precursors were tested by TGA/DTA. The samples were heated up to 1000 °C in air with a rate of 10 °C/min, using a TGA/SDTA 851e METTLER TOLEDO. The structure and crystallite sizes were tested by X-ray diffractometer (XRD) in the 2θ range 25–60° using CuK α radiation ($\lambda = 0.15405$ nm). The type of XRD is SHIMADZU Co.Tokyo Japan. The crystallite sizes are calculated using Scherrer's relationship.

$$D = k\lambda/B \cos \theta$$

where ' D ' is the average diameter in nm, ' k ' is the shape factor, ' B ' is the broadening of the diffraction line measured half of its maximum intensity in 'radians', ' λ ' is the wave length of X-ray and ' θ ' is the Bragg's diffraction angle. The crystallite sizes of the samples are estimated from the line width of the (420) XRD peaks. Infrared spectra were recorded using a Nicolet-510 IR spectrometer on samples palletized with KBr. Mössbauer spectrum was recorded at 295 K by using a computerized Oxford MS-500 Mössbauer spectrometer of the electromechanical type in constant acceleration mode. A ^{57}Co source in a rhodium matrix was used in a continuously distributed hyperfine magnetic field. A 25 μm thick high purity alpha iron foil was used for calibration. The experimental data were analyzed with a standard least squared fitting program assuming Lorentzian line shapes. Magnetic measurements were carried out at room temperature using a vibrating sample magnetometer (VSM) (Digital Measurement System JDM-13) with a maximum magnetic field of 10000 Oe. Here, nanosized powders of 100 mg were poured in a plastic tube that was installed in the device.

Results and discussion

DTA and TG

DTA and TGA curves of the precursor of $\text{BiY}_2\text{Fe}_5\text{O}_{12}$ are shown in Fig. 1. DTA plot shows an endothermic peak at 300 °C which is accompanied with large weight loss. It is probably due to decomposition of the surfactant of the citric acid. The process of decomposition of the citric acid is completed at 440 °C, and accordingly we preheat the samples at 450 °C for 1 h to burn out the surfactant.

Following the exothermic peaks, some small exothermic peaks appear in the DTA curve between 650 °C and 850 °C which can be due to formation of the $\text{BiY}_2\text{Fe}_5\text{O}_{12}$.

X-ray diffraction

Figure 2 shows the X-ray diffraction patterns of $\text{BiY}_2\text{Fe}_5\text{O}_{12}$ calcined in the range of 700–1000 °C. Fig. 1a

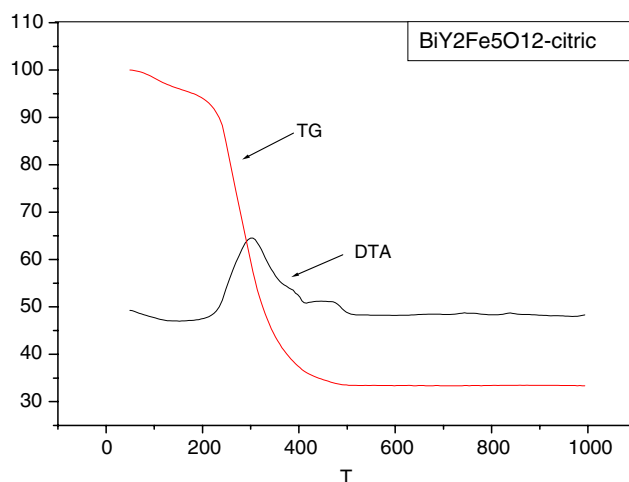


Fig. 1 TG and DTA plots of $\text{BiY}_2\text{Fe}_5\text{O}_{12}$ precursor

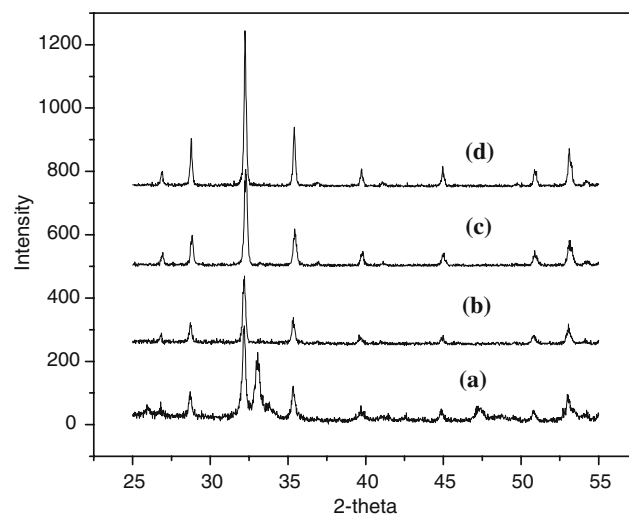
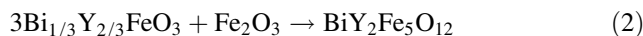
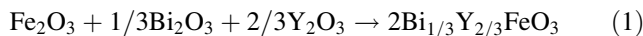


Fig. 2 XRD patterns of $\text{BiY}_2\text{Fe}_5\text{O}_{12}$ nanoparticles calcined at: (a) 700 °C, (b) 850 °C, (c) 920 °C, (d) 1000 °C

shows that at 700 °C the XRD pattern can be attributed to the garnet phase of $\text{BiY}_2\text{Fe}_5\text{O}_{12}$ and $\text{Bi}_{1/3}\text{Y}_{2/3}\text{FeO}_3$ with the perovskite structure. The latter is the intermediate compound in the process of the crystallization. The $\text{BiY}_2\text{Fe}_5\text{O}_{12}$ is formed at 850 °C, which is a single garnet (Fig. 1b). The forming process of the $\text{BiY}_2\text{Fe}_5\text{O}_{12}$ can be expressed by the following chemical reactions:



The crystallite sizes of $\text{BiY}_2\text{Fe}_5\text{O}_{12}$ are increased apparently with increasing the annealing temperature from 850 °C to 1000 °C (Fig. 1c and d).

The X-ray diffraction patterns of $\text{BiY}_2\text{Cr}_x\text{Fe}_{5-x}\text{O}_{12}$ ($x = 0, 0.05, 0.1, 0.2, 0.3, 0.4$) nanoparticles calcined at

850 °C are shown in Fig. 3. The XRD patterns of the samples are all consistent with standard XRD card of the samples when the Cr^{3+} content x is smaller than or equal to 0.3. The perovskite phase appear in the XRD pattern when $x = 0.4$ which means that we can obtain single-phase garnet nano-particles only when $x \leq 0.3$ [5, 6].

Figure 4 is the dependence of the crystalline size and the Cr^{3+} contents of $\text{BiY}_2\text{Cr}_x\text{Fe}_{5-x}\text{O}_{12}$ nanoparticles calcined at 850 °C, 920 °C, 1000 °C. Substitution of a mount of Fe^{3+} ions by Cr^{3+} ions has no influence on the crystallite sizes of samples, which maybe relate to the reason that the ionic radius of Cr^{3+} (0.63 Å) is close to that of Fe^{3+} (0.65 Å). The crystallite size of the samples increased apparently with increasing calcined temperature.

Magnetic studies

The magnetic hysteresis cures of $\text{BiY}_2\text{Fe}_5\text{O}_{12}$ and $\text{BiY}_{1.2}\text{Cr}_{0.1}\text{Fe}_{4.9}\text{O}_{12}$ samples are shown in Fig. 5. The special saturation magnetization (M_s) of the samples at

room temperature was obtained from the hysteresis curve for each sample, and the value of coercivity (H_c) and remanence saturation magnetization (M_r) are all zero. The dependence of the special saturation magnetization on the Cr^{3+} content is plotted in Fig. 6.

As can be seen there is a increase of the special saturation magnetization as the Cr^{3+} content x is smaller than 0.1 and it reach the peak when $x = 0.1$. The biggest value of the M_s of $\text{BiY}_2\text{Cr}_x\text{Fe}_{5-x}\text{O}_{12}$ is 26.98 emu/g and it is 23.82 emu/g when $x = 0.0$. Saturation magnetization decrease with the increase of x when $x > 0.1$.

Garnet has the composition $\text{A}_3\text{B}_2\text{B}'_3\text{O}_{12}$ (cubic space group, Ia3d),with eight formula units per cell. In the case of $\text{BiY}_2\text{Fe}_5\text{O}_{12}$, the A = Y^{3+} , Bi^{3+} site is eight-fold dodecahedral coordinated(c site), The B = Fe^{3+} site six-fold octahedral (a site) and the B' = Fe^{3+} site four-fold tetrahedral (d site). Y^{3+} , Bi^{3+} are diamagnetic and $5 \mu_B$ ($T = 0 \text{ K}$) per formula unit results from negative super-exchange (antiferromagnetic) interactions are dominant to a–a and d–d interactions.

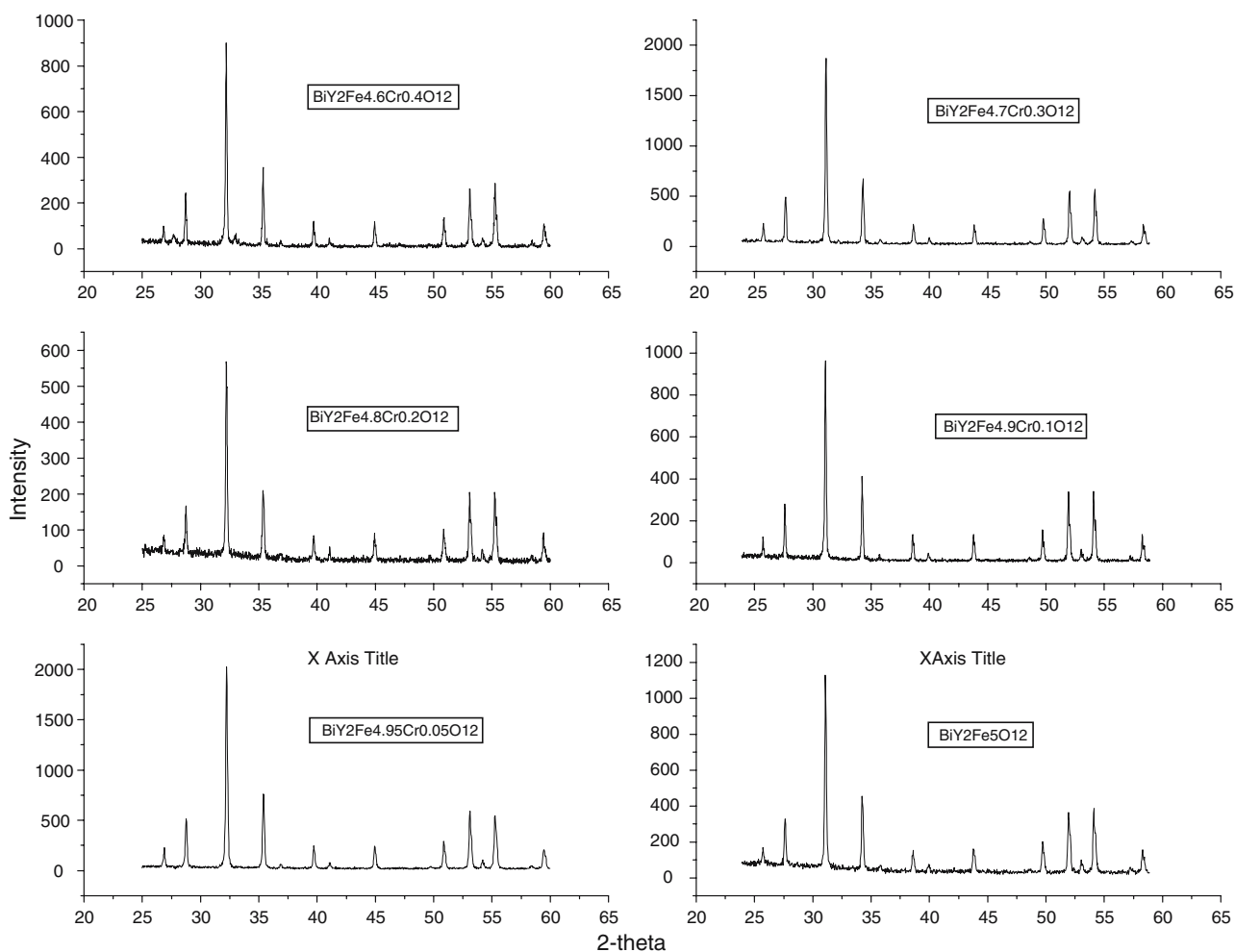


Fig. 3 XRD patterns of $\text{BiY}_2\text{Cr}_x\text{Fe}_{5-x}\text{O}_{12}$ nanoparticles calcined at 850 °C

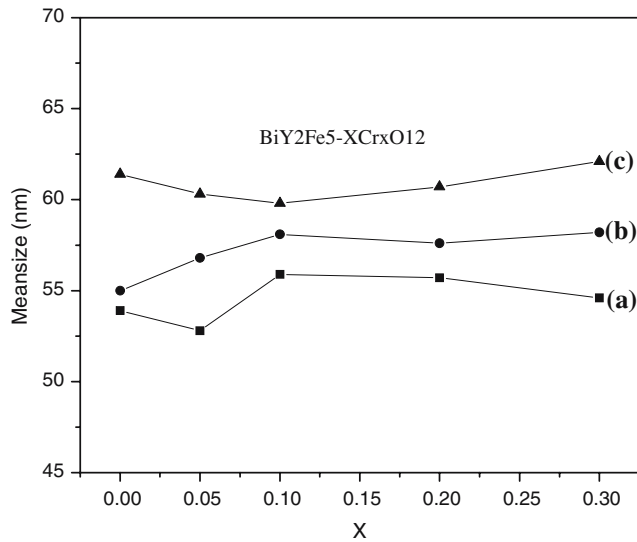


Fig. 4 The relation between the crystallite sizes (nm) and the Cr^{3+} content of $\text{BiY}_2\text{Cr}_x\text{Fe}_{5-x}\text{O}_{12}$ nanocrystals calcined at 850 °C, 920 °C, 1000 °C

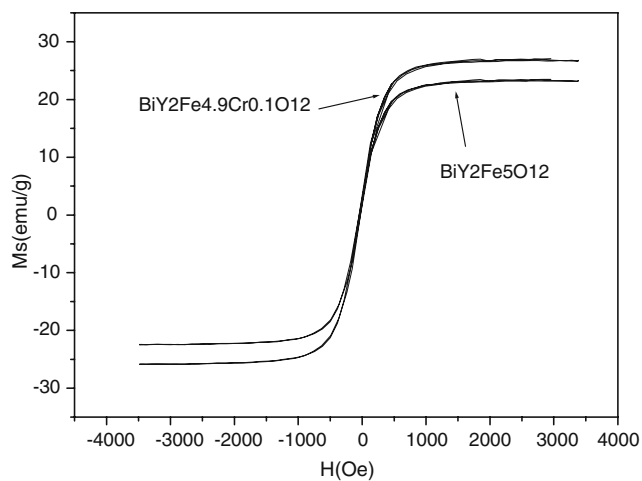


Fig. 5 The hysteresis loop of $\text{BiY}_2\text{Fe}_5\text{O}_{12}$ and $\text{BiY}_{1.2}\text{Cr}_{0.1}\text{Fe}_{4.9}\text{O}_{12}$ nanoparticles calcined at 850 °C

The magnetic structure of $\text{BiY}_2\text{Cr}_x\text{Fe}_{5-x}\text{O}_{12}$ can be understood with the framework of the sub-lattice magnetization model of Dionne [7]. According to this model, the magnetization of $\text{BiY}_2\text{Cr}_x\text{Fe}_{5-x}\text{O}_{12}$, $\{\text{BiY}_2\}[\text{Fe}_{2-y}\text{Cr}_y](\text{Fe}_{3-z}\text{Cr}_z)\text{O}_{12}$ ($\{\}$ = c sub-lattice, $[\]$ = a sub-lattice, $()$ = d sub-lattice), is given by

$$M_{\text{total}}(T, H_{\text{app}}) = M_d(T, H_{\text{app}}) - M_a(T, H_{\text{app}})$$

where H_{app} is the applied magnetic field; T is the temperature; M_d and M_a , the sub-lattice magnetization of ‘d’ and ‘a’ sub-lattice.

Figure 5 shows that the saturation magnetization (M_s) of $\text{BiY}_2\text{Cr}_x\text{Fe}_{5-x}\text{O}_{12}$ increased apparently as x increases

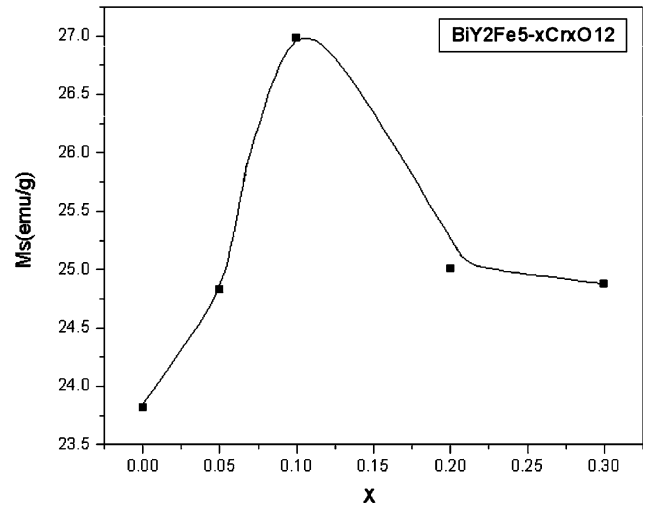


Fig. 6 The dependence of saturation magnetization of $\text{BiY}_2\text{Cr}_x\text{Fe}_{5-x}\text{O}_{12}$ nanocrystals on the Cr^{3+} content

from 0 to 0.1. The magnetic moment of Cr^{3+} and Fe^{3+} are $3 \mu_B$ and $5 \mu_B$ individually. So the Cr^{3+} ions maybe enter into a sub-lattice completely for $0 \leq x \leq 0.1$. Saturation magnetization (M_s) decrease as $x > 0.1$, which indicate that, at higher concentrations, some of the Cr^{3+} ions begin to enter into d sub-lattice. The plot along with the Cr content show that Cr^{3+} ions have preference to octahedral site, but the ions will enter into the tetrahedral site for higher Cr concentration which can be understood by the effects of the disordering [8].

The Mössbauer spectrum of $\text{BiY}_2\text{Fe}_5\text{O}_{12}$ and $\text{BiY}_{1.2}\text{Cr}_{0.1}\text{Fe}_{4.9}\text{O}_{12}$ at room temperature are shown in Fig. 7. The spectrums for the two specimens show the presence of two sextets.

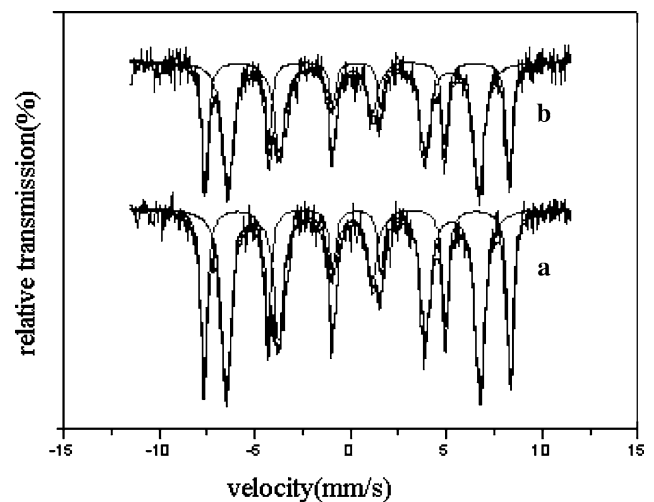


Fig. 7 Mössbauer spectrum. (a) $\text{BiY}_2\text{Fe}_5\text{O}_{12}$. (b) $\text{BiY}_{1.2}\text{Cr}_{0.1}\text{Fe}_{4.9}\text{O}_{12}$, calcined at 850 °C

Table 1 The Mössbauer parameters for $\text{BiY}_2\text{Fe}_5\text{O}_{12}$ and $\text{BiY}_{1.2}\text{Cr}_{0.1}\text{Fe}_{4.9}\text{O}_{12}$ nanocrystals

Parameters	Specimens	
	$\text{BiY}_2\text{Fe}_5\text{O}_{12}$	$\text{BiY}_{1.2}\text{Cr}_{0.1}\text{Fe}_{4.9}\text{O}_{12}$
δ (a) (mm/s)	0.39 ± 0	0.39 ± 0
δ (d) (mm/s)	0.17 ± 0	0.18 ± 0
ΔE (a) (mm/s)	0.02 ± 0.01	0.03 ± 0.01
ΔE (d) (mm/s)	0.05 ± 0	0.05 ± 0
B (a) (kOe)	496.3 ± 0.3	492.4 ± 0.4
B (d) (kOe)	410.6 ± 0.4	406.4 ± 0.5
Area (a)	37.2%	35.4%
Area(d)	62.8%	64.6%

The Mössbauer parameters for $\text{BiY}_2\text{Fe}_5\text{O}_{12}$ and $\text{BiY}_{1.2}\text{Cr}_{0.1}\text{Fe}_{4.9}\text{O}_{12}$ nanocrystals are listed in Table 1. δ , ΔE , B and Area represent isomer shift, quadruple shift, hyperfine field and percent of absorption area. Table 1 illustrates that the δ values of a-sites is larger than that of d-sites. This conclusion has been proved by many literatures [9–11]. The values of ΔE indicate the degree of deviating from cubic symmetrical structure. The absolute values of ΔE of octahedral site are increased with the increasing Cr^{3+} ions content which means the asymmetrical electric fields surrounding the Mössbauer nucleus are strengthened along with the increasing doped ions. But the absolute values of ΔE of tetrahedral site ($\Delta E(d)$) don't change and it indicate that no Cr^{3+} ions enter into tetrahedral site when $x = 0.1$.

The hyperfine magnetic field at iron nucleus originates mainly from the net atomic spin density through the Fermi contact potential. The net spin density is affected by the interaction of the electronic wave functions of the Mössbauer ion Fe^{3+} with the surrounding ions. The value of B (a, d) of $\text{BiY}_2\text{Fe}_5\text{O}_{12}$ is larger than that of $\text{BiY}_{1.2}\text{Cr}_{0.1}\text{Fe}_{4.9}\text{O}_{12}$ [10]. This may be attributed to that the magnetic super-interaction is decreased for the Cr^{3+} ions substitution for Fe^{3+} ions in sub-lattice sites [12].

From the percent of the absorption area of the Mössbauer spectra, we can decide the cation distribution. The fraction of Fe^{3+} ions at the tetrahedral d sites and octahedral a sites were determined using the area of Mössbauer spectra. For stoichiometric ferrite it is easy to estimate the cation distribution, but it becomes rather difficult for mixed ferrites, since they contain mixtures of more than one cation other than iron. However, if the metal ions have an exclusive preference for any particular site in the garnet, then it is possible to estimate the cation site in the mixed ferrites. For $\text{BiY}_{1.2}\text{Cr}_{0.1}\text{Fe}_{4.9}\text{O}_{12}$ ferrite nanocrystals, the

absorption area of octahedral a sites is larger than that of $\text{BiY}_2\text{Fe}_5\text{O}_{12}$ and the change of the ratio of the sites is consistent to the doped Cr^{3+} ions content. This confirm that Cr^{3+} ions have the insensitive preference for the a sites and they enter into octahedral a sites completely for $x \leq 0.1$. Using the area percent data, the cations distribution of $\text{BiY}_{1.2}\text{Cr}_{0.1}\text{Fe}_{4.9}\text{O}_{12}$ ferrite nanocrystal can explain the phenomenon that substitution of the Cr^{3+} ions for Fe^{3+} ions can enhance the magnetic properties of garnet nanocrystals [13].

Conclusions

A series of c have been synthesized by sol-gel method. We studied the process of crystallization of $\text{BiY}_2\text{Fe}_5\text{O}_{12}$ with DTA/TG and XRD analyses. From these results it can be concluded that sintering above 850 °C is necessary to obtain a single garnet phase of nanocrystalline. The crystallite sizes of $\text{BiY}_2\text{Cr}_x\text{Fe}_{5-x}\text{O}_{12}$ ferrite nanocrystals vary with the heat treatment temperatures. However variation of Cr^{3+} ions content don't influence the crystallite sizes of $\text{BiY}_2\text{Cr}_x\text{Fe}_{5-x}\text{O}_{12}$. The saturation magnetization of $\text{BiY}_2\text{Fe}_{5-x}\text{Cr}_x\text{O}_{12}$ increases with the increase of x when $x < 0.1$, and it achieve the peak when $x = 0.1$. While the value of M_s decrease with the increase of x when $x > 0.1$. Mossbauer spectrum confirms that Cr^{3+} enter into a site completely when $x \leq 0.1$.

Acknowledgements This work is supported by National Natural Science Foundation of China (NSFC) (Grant No. 50372025 and 50572033).

References

1. Rehspringer J-L, Bursik J, Niznansky D (2000) J Magn Magn Mater 211:291
2. Zhao H, Zhou J, Bai Y (2004) J Magn Magn Mater 280:208
3. Jeon YH, Lee JW, Oh JH (2004) Phys Stat Sol(a) 201(8):1893
4. Amighian J, Hasanpour A, Mozaffari M (2004) Phys Stat Sol(c) 1(7):1769
5. Todorovsky DS, Todorovska RV, Groudeva-Zotova St (2002) Mater Lett 55:41
6. Ristic M, Nowik I, popvic S (2003) Mater Lett 57:2584
7. Dionne GF (1970) J Appl Phys 41:4874
8. Thongmee S, Winotaia P, Tang IM (1999) Solid State Commn 109:471
9. Fabien G, Stephane M (2001) J Magn Magn Mater 234:409
10. Chiara M, Vincenzo B (2004) Chem Mater 16:1232
11. Rodic D, Mitric M, Tellgren R (1999) J Magn Magn Mater 191:137
12. Ristic M, Nowik I, popvic S (2003) Mater Lett 57:2584
13. Mahdi S, Lataifeha, Sami Mahmoodb (2002) Physica B 321:143